



A EUROPEAN JOURNAL

CHEMPHYSICHEM

OF CHEMICAL PHYSICS AND PHYSICAL CHEMISTRY

Accepted Article

Title: Thiazolocatechol: Electron-withdrawing Catechol Anchoring Group for Dye-Sensitized Solar Cells

Authors: Tomohiro Higashino, Hitomi Iiyama, Yuma Kurumisawa, and Hiroshi Imahori

This manuscript has been accepted after peer review and appears as an Accepted Article online prior to editing, proofing, and formal publication of the final Version of Record (VoR). This work is currently citable by using the Digital Object Identifier (DOI) given below. The VoR will be published online in Early View as soon as possible and may be different to this Accepted Article as a result of editing. Readers should obtain the VoR from the journal website shown below when it is published to ensure accuracy of information. The authors are responsible for the content of this Accepted Article.

To be cited as: *ChemPhysChem* 10.1002/cphc.201900342

Link to VoR: <http://dx.doi.org/10.1002/cphc.201900342>

WILEY-VCH

www.chemphyschem.org



Thiazolocatechol: Electron-withdrawing Catechol Anchoring Group for Dye-Sensitized Solar Cells

Tomohiro Higashino,^[a] Hitomi Iiyama,^[a] Yuma Kurumisawa,^[a] and Hiroshi Imahori*^[a,b]

Abstract: Anchoring groups adopting a five-membered bidentate chelating are attractive to realize a high power conversion efficiency (η) and long-term durability in dye-sensitized solar cells (DSSCs). In this regard, we chose catechol as an anchoring group that can adopt the chelating. However, the DSSCs with catechol-based sensitizers have never exceeded an η -value of 2%. These poor photovoltaic performances may be associated with the electron-donating ability of the hydroxy groups in catechol. Considering these, we envisioned that fusing an electron-withdrawing thiazole moiety with a catechol anchoring group would improve its photovoltaic performance. Herein, we report a push-pull porphyrin sensitizer **ZnPTC** with a thiazolocatechol anchoring group. The DSSC with **ZnPTC** exhibited $\eta = 4.87\%$. This value is the highest ever reported for catechol-anchor based DSSCs. Meanwhile, the long-term cell durability was not improved, although the robust anchoring properties were attained under harsh conditions.

Introduction

In recent years, the development of anchoring groups to bind organic molecules and metal oxides have been actively explored for heterogeneous catalysts and photoelectrochemical cells, which are promising technologies to realize sustainable energy systems. In this regard, photoelectrochemical cells, which convert solar energy into electricity or useful chemicals, have attracted much attention.^[1,2] In particular, dye-sensitized solar cells (DSSCs) are a fascinating candidate for an alternative to conventional silicon-based solar cells because of their potential low-cost production and a high power conversion efficiency (η).^[1] Since the epoch-making paper by Grätzel et al. in 1991,^[3a] diverse ruthenium^[3] and organic sensitizers^[4] have been assessed for their applications to DSSCs. Among various kinds of sensitizers, porphyrins are attractive candidates because of their intense absorption in the visible region and easily modulated structures.^[5] Push-pull porphyrin sensitizers have achieved an excellent light-harvesting ability and demonstrated high η -values more than 10%.^[6]

To date, carboxylic acid is the most widely used anchoring

group for DSSCs owing to its simple synthesis and sufficient binding ability to TiO₂ in organic solvents. Nevertheless, carboxylic acid tends to detach from TiO₂ during the cell operation under illumination and in the presence of water. To attain the long-term durability of the DSSCs toward their practical application, stable anchoring groups have been explored.^[7] In this connection, we previously reported that push-pull porphyrin sensitizers with tropolone^[8a] and hydroxamic acid^[8b] anchoring groups attained both high η -values and long-term durability of the DSSCs. In contrast to the possible binding mode of four-membered bidentate chelating for carboxylic acid, tropolone and hydroxamic acid anchoring groups can adopt a five-membered bidentate chelating as possible binding modes (Figure 1a). Thus, utilization of anchoring groups possessing a five-membered bidentate chelating would be an effective means to realize both high η -value and long-term durability. Along this line, we focused on catechol as an anchoring group that is known to adopt a five-membered bidentate chelating.^[9]

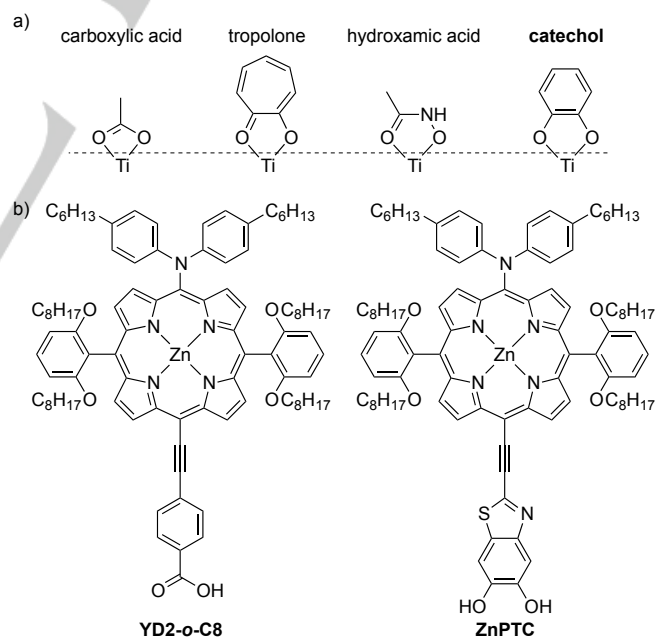


Figure 1. a) Possible binding modes for anchoring groups on TiO₂. b) Molecular structures of porphyrin sensitizers in this study.

Although several organic sensitizers with catechol anchoring groups have been tested,^[9b,10] their photovoltaic performances have never exceeded an η -value of 2%.^[10a] Porphyrin sensitizers with a catechol anchoring group have appeared, but their photovoltaic performances are also limited to less than an η -value of 1%.^[10e] These poor photovoltaic performances may be

[a] Dr. T. Higashino, H. Iiyama, Y. Kurumisawa, Prof. Dr. H. Imahori
Department of Molecular Engineering
Graduate School of Engineering, Kyoto University
Nishikyo-ku, Kyoto 615-8510 (Japan)
E-mail: imahori@scl.kyoto-u.ac.jp

[b] Prof. Dr. H. Imahori
Institute for Integrated Cell-Material Sciences (WPI-iCeMS)
Kyoto University
Sakyo-ku, Kyoto 606-8501 (Japan)

Supporting information for this article is given via a link at the end of the document.

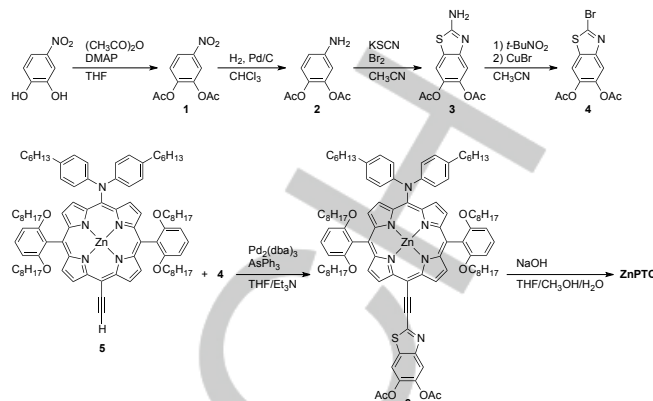
associated with the electron-donating ability of the hydroxy groups in catechol. In terms of molecular design for excellent sensitizers in DSSCs, the electron-donating nature of the catechol group is inappropriate for a fast electron injection process from the excited sensitizer to TiO₂ as well as efficient intramolecular charge-transfer interaction in push-pull structures. Bearing these in mind, we expected that fusing an electron-withdrawing thiazole moiety with a catechol anchoring group would improve photovoltaic performance.

Herein, we report a thiazolocatechol as a new catechol anchoring group with an electron-withdrawing thiazole moiety. We anticipated the improvement of the light-harvesting ability, photovoltaic performances, and robust anchoring properties owing to its π -expansion and enhanced electron-withdrawing nature arising from the thiazole-fused structure. To examine the effect of the thiazolocatechol anchoring group, selected as the basic motif was **YD2-o-C8**, which is one of the best sensitizers in DSSCs.^[6b] The carboxyphenyl group of **YD2-o-C8** was replaced with the thiazolocatechol anchoring group to give a push-pull porphyrin sensitizer **ZnPTC** (Figure 1b). Their optical, electrochemical, and photovoltaic properties were described in this paper.

Results and Discussion

Synthesis and characterization

The synthetic scheme of **ZnPTC** is shown in Scheme 1. The reaction of 4-nitrocatechol with acetic acid anhydride gave acetylated catechol **1**. After reduction of the nitro group of **1**, the reaction of **2** with potassium thiocyanate provided 2-aminothiazolocatechol **3**. Sandmeyer reaction of **3** afforded 2-bromothiazolocatechol **4**. In the next step, we synthesized the porphyrin core **5** according to the literature.^[6b] Sonogashira coupling of **5** with **4** gave the porphyrin intermediate **6**. Finally, hydrolysis of **6** with an excess amount of NaOH furnished the push-pull porphyrin sensitizer **ZnPTC** with the thiazolocatechol anchoring group. All the compounds were fully characterized by high-resolution mass spectrometry and ¹H and ¹³C NMR and IR spectroscopies (Figures S1–S5). Although the ¹H NMR spectrum of **ZnPTC** in CDCl₃ was broad, the signals became sharp by adding [D₅]-pyridine into the CDCl₃ solution (Figure S5). These results indicate the aggregation tendency of **ZnPTC**, which may be ascribed to the intermolecular coordination of hydroxy moieties on the thiazolocatechol group to the zinc metal of the porphyrin core. **YD2-o-C8** was also prepared as a control compound according to the literature.^[6b]



Scheme 1. Synthesis of **ZnPTC**.

Absorption, Fluorescence, and Electrochemistry

The UV-visible absorption spectra of **ZnPTC** and **YD2-o-C8** in THF are depicted in Figure 2a. The Soret and Q-bands of **ZnPTC** are shifted toward longer wavelengths compared to those of **YD2-o-C8**. This improved light-harvesting ability of **ZnPTC** can be rationalized by higher electron-withdrawing nature of the thiazolocatechol group than that of the carboxyphenyl group. The emission spectrum of **ZnPTC** in THF reveals a red-shifted peak at 677 nm relative to that of **YD2-o-C8** (669 nm, Figure 2b). By using the crossing of the normalized absorption and fluorescence spectra, the optical HOMO–LUMO gaps were estimated to be 1.86 eV for **ZnPTC** and 1.89 eV for **YD2-o-C8** (Figure S6). The fluorescence lifetimes (τ_F) were determined by using time-correlated single photon counting (TCSPC) method. **ZnPTC** ($\tau_F = 1.3$ ns) shows a slightly shorter value than **YD2-o-C8** ($\tau_F = 1.6$ ns), indicating that the thiazolocatechol anchoring group has no significant impact on the excited-state dynamics. Since the decaying processes are much slower than the typical electron injection processes from the excited singlet state to TiO₂,^[11] they would not affect the η -values (vide infra).

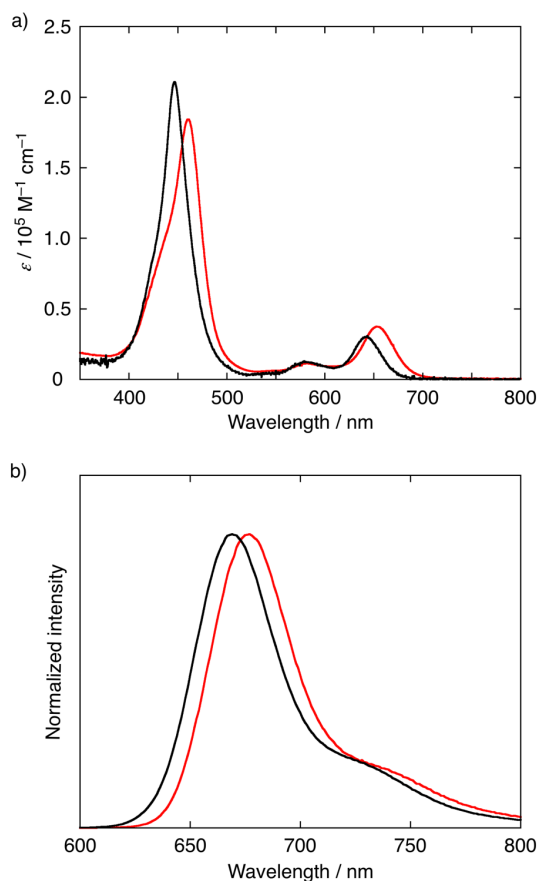


Figure 2. a) UV-visible absorption and b) normalized emission spectra of **ZnPTC** (red) and **YD2-o-C8** (black) in THF. For the emission measurement, wavelengths of Soret band maxima were used for the excitation.

The electrochemical properties of **ZnPTC** (versus NHE) in THF were studied by using cyclic voltammetry (CV) and differential pulse voltammetry (DPV). As an electrolyte tetrabutylammonium hexafluorophosphate ($n\text{-Bu}_4\text{NPF}_6$) was employed (Figure S7 and Table 1). The first oxidation potential (E_{ox}) of **ZnPTC** is shifted slightly to a negative direction with respect to **YD2-o-C8**, whereas their first reduction potentials (E_{red}) are identical. These results are consistent with the higher electron-withdrawing nature of the thiazolocatechol group than that of the carboxyphenyl group. The electrochemical HOMO-LUMO gaps were calculated from the E_{ox} and E_{red} values. The HOMO-LUMO gap of **ZnPTC** (1.97 eV) is slightly smaller compared to that of **YD2-o-C8** (2.00 eV), which matches with the tendency on the HOMO-LUMO gaps determined optically. On a basis of the measurements, free energy changes for the electron transfer (ET) processes, i.e., electron injection (ΔG_{inj}) and dye regeneration (ΔG_{reg}), were calculated.^[8b] Considering sufficient free energy changes for the ET processes (< -0.19 eV), efficient ET is possible for their processes.

Table 1. Redox potentials and free energy changes of **ZnPTC** and **YD2-o-**

C8.

	$E_{\text{ox1}}^{[a]}$ [V]	$E_{\text{red1}}^{[a]}$ [V]	$E_{\text{g}}^{\text{opt}}$ [eV]	E_{ox}^* ^[b] [V]	$\Delta G_{\text{inj}}^{[c]}$ [eV]	$\Delta G_{\text{reg}}^{[d]}$ [eV]
ZnPTC	0.76	-1.21	1.86	-1.10	-0.60	-0.19
YD2-o-C8 ^[e]	0.79	-1.21	1.89	-1.10	-0.60	-0.22

[a] Obtained by using DPV (vs. NHE). [b] Obtained by adding $E_{\text{g}}^{\text{opt}}$ to E_{ox1} . [c] Free energy change for electron transfer from the singlet excited state of the porphyrin to the conduction band (CB) of TiO_2 (-0.5 V vs. NHE). [d] Free energy change for electron transfer from tris(bipyridyl) Co^{III} redox couple (+0.57 V vs. NHE) to the oxidized porphyrin. [e] From ref 12.

We carried out calculations for the simplified porphyrins using density functional theory (DFT) at the B3LYP/6-31G(d) level to obtain information on the structural and electronic properties of the porphyrins (Figure S8). Both the porphyrins show similar ground-state geometry. The calculated HOMO-LUMO gaps are 2.30 eV for **ZnPTC** and 2.32 eV for **YD2-o-C8**, which agree with the trends on the HOMO-LUMO gaps obtained optically and electrochemically. The orbital distribution on the thiazolocatechol group in the LUMO of **ZnPTC** is smaller than that on the carboxyphenyl group in the LUMO of **YD2-o-C8**. Since the orbital distributions of LUMO around an anchoring group are known to affect the electronic coupling between $^1\text{ZnP}^*$ and the 3d orbital of TiO_2 ,^[13] the electron injection of **ZnPTC** on TiO_2 may be slower than that of **YD2-o-C8** on TiO_2 (vide infra). In contrast, the orbital distribution on the thiazolocatechol group in the HOMO of **ZnPTC** is larger than that on the carboxyphenyl group in the HOMO of **YD2-o-C8**, accelerating the charge recombination (CR) from electron in the CB of TiO_2 to ZnP^{*+} for **ZnPTC** (vide infra).

Binding structure

We examined the binding property of the thiazolocatechol anchoring group on TiO_2 . A TiO_2 electrode was immersed in a 1:4 mixture of THF and ethanol containing porphyrin (0.2 mM) to give a porphyrin-sensitized TiO_2 electrode. The porphyrin surface coverage (Γ) on the TiO_2 surface was estimated by measuring the porphyrin absorbance at 640 nm on the TiO_2 electrode in comparison with that of **YD2-o-C8** (Figure 3). During the immersion, **ZnPTC** and **YD2-o-C8** reach the saturated surface coverages on TiO_2 in 3 and 2 h, respectively. It is noteworthy that the saturated Γ value of **ZnPTC** (1.3×10^{-10} mol cm^{-2}) exceeds that of **YD2-o-C8** (8.2×10^{-11} mol cm^{-2}). Although the molecular structures of the two porphyrins are almost identical, their anchoring groups affect the Γ values significantly. The high Γ value of **ZnPTC** may be related with the high aggregation tendency of **ZnPTC**.

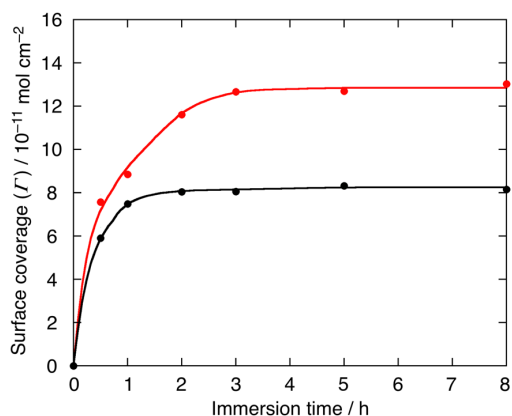


Figure 3. Adsorption profiles of porphyrins **YD2-o-C8** (black) and **ZnPTC** (red) versus immersion time. The porphyrin surface coverages (Γ) were determined for the TiO_2 electrodes with no light-scattering layers.

In the next step, we examined the binding structure of the thiazolocatechol anchoring group on TiO_2 . X-ray photoelectron spectroscopic measurements were performed for catechol and **ZnPTC** (Figures S9 and S10). The O1s photoelectron spectrum of the catechol powder displays a peak at 532.1 eV, which is originated from the OH moieties. After adsorption of catechol on TiO_2 , the spectrum displays two peaks at 531.4 and 530.2 eV, which are assigned to the O atoms of the C–O–Ti moiety and TiO_2 . The shift of the corresponding binding energies from 532.1 eV to 531.4 eV together with appearance of the single peak at 531.4 eV suggests the bidentate adsorption mode of catechol to TiO_2 .^[14] The O1s photoelectron spectrum of the **ZnPTC** powder illustrates two peaks at 532.4 and 531.5 eV, arising from the oxygen atoms of the OH moieties in the thiazolocatechol anchoring group and of the octyloxy moieties. After adsorption of **ZnPTC** on TiO_2 , the spectrum shows three peaks at 531.3, 530.3, and 529.4 eV, which are assigned to the oxygen atoms of the octyloxy moieties, of TiO_2 , and of the C–O–Ti moiety. From the X-ray photoelectron spectroscopic measurements, we can conclude that the binding mode of thiazolocatechol moiety on TiO_2 is symmetrical bidentate coordination, i.e., bidentate chelating and/or bidentate bridging modes.

Solar cell properties

The device performances of DSSCs were evaluated in standard AM1.5 conditions. Tris(bipyridyl)cobalt^{III/II} complexes were used as the redox couple. To optimize the cell performance, we first examined the effect of immersion time on the photovoltaic properties without co-adsorbent (Figure S11). The DSSC with **ZnPTC** exhibits a highest η -value of 3.7% in an immersion time of 0.5 h. The decreasing trend after reaching the maximum suggests the aggregation behavior of **ZnPTC** on TiO_2 , which agrees with the higher surface coverage of **ZnPTC** than **YD2-o-C8** (*vide supra*). By fixing the immersion time at 0.5 h, we also evaluated the effect of chenodeoxycholic acid (CDCA), a co-adsorbent for the suppression of porphyrin aggregation on TiO_2 . Indeed, the co-adsorption of CDCA improved the cell performance. A maximal η -value of 4.87% was attained with 20

equivalents of CDCA (Figure S12). The use of the large excess amount of CDCA for improving the cell performance also supports the strong aggregation behavior of **ZnPTC** on TiO_2 . The highest value ($\eta = 4.87\%$) of the DSSC with **ZnPTC** under our optimized conditions is significantly low compared to that with **YD2-o-C8** ($\eta = 9.93\%$) under the optimized conditions without the addition of CDCA (Figure 4 and Table 2). Notwithstanding, as far as we know, the DSSC with **ZnPTC** attains the record efficiency of the DSSCs based on porphyrin sensitizers with a catechol anchoring group (0.8%)^[10e] and even organic sensitizers with a catechol anchoring group (1.6%).^[10a]

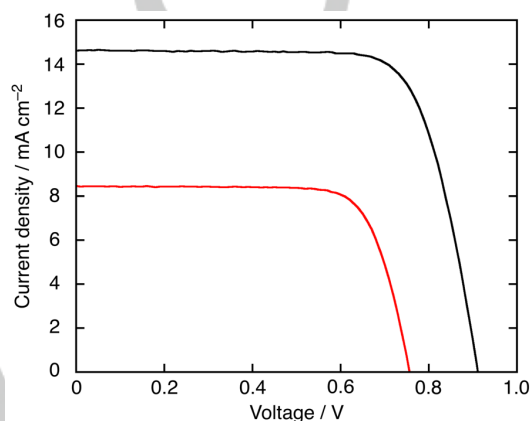


Figure 4. Photocurrent-voltage curves of the DSSCs with **YD2-o-C8** (black) and **ZnPTC** (red) under the optimized conditions.

Table 2. Photovoltaic performances of **YD2-o-C8** and **ZnPTC**.^[a]

	J_{sc} [mA cm^{-2}]	V_{oc} [V]	ff ^[b]	η [%]
ZnPTC ^[c]	8.46 (8.23 \pm 0.12)	0.757 (0.763 \pm 0.006)	0.760 (0.754 \pm 0.009)	4.87 (4.73 \pm 0.07)
YD2-o-C8 ^[d]	14.6 (14.2 \pm 0.3)	0.912 (0.897 \pm 0.010)	0.746 (0.743 \pm 0.007)	9.93 (9.49 \pm 0.23)

[a] Values represent solar cell parameters exhibiting the best η -value. Values in bracket show average values obtained from eight different experiments. [b] Fill factor. [c] Immersion time: 0.5 h, chenodeoxycholic acid (CDCA): 20 equiv. [d] Immersion time: 3 h, CDCA: 0 equiv.

The absorption spectra of the porphyrin-adsorbed TiO_2 electrodes and the action spectra of the DSSCs are shown in Figure 5. Although the **ZnPTC**-sensitized TiO_2 electrode displays red-shifted absorption, the photocurrent generation efficiency (incident photon-to-current efficiency (IPCE)) of the DSSC based on **ZnPTC** are lower than those with **YD2-o-C8** in all the wavelength regions. The IPCE value is calculated from the following equation: $\text{IPCE} = \text{LHE} \times \phi_{inj} \times \eta_{col}$, where LHE (light-

harvesting efficiency) is the number of adsorbed photons per incident photon, ϕ_{inj} is the efficiency of electron injection, and η_{col} is the efficiency of charge collection. Because the LHE of **ZnPTC** and **YD2-o-C8** are comparable (Figure 5a), the ϕ_{inj} and/or η_{col} of **ZnPTC** should be lower than those of **YD2-o-C8**. Although the aggregation of **ZnPTC** on TiO_2 is suppressed by co-adsorption of the large excess amount of CDCA to some extent, the ϕ_{inj} value would be low compared to that of the DSSC based on **YD2-o-C8**, considering the smaller orbital distributions of the thiazolocatechol anchoring group in the LUMO in addition to the aggregation-induced fast quenching of $^1\text{ZnP}^*$ on TiO_2 . To examine the ET process from the redox shuttle to the oxidized porphyrin, microsecond time-resolved transient absorption (TA) measurements were performed for the porphyrin-sensitized TiO_2 films using neat acetonitrile and cobalt electrolyte solutions (Figure S13). We monitored the decay profiles of characteristic absorption at 800 nm corresponding to ZnP^{2+} , which was confirmed by the UV/Vis absorption measurements of the chemically oxidized porphyrins (Figure S14). The lifetime of ZnP^{2+} in the absence of the cobalt redox shuttle for **ZnPTC** (15.3 μs) was significantly shorter than that for **YD2-o-C8** (40.7 μs), which shows the faster CR process between ZnP^{2+} and electron in the CB of TiO_2 for **ZnPTC**. From the lifetimes of ZnP^{2+} in the absence and presence of the cobalt redox shuttle, the dye regeneration efficiencies (ϕ_{reg}) can be estimated to be 72% for **ZnPTC** and 73% for **YD2-o-C8**. The similar ϕ_{reg} values suggest that the difference in the IPCE values at least to some extent results from fast CR processes from the electron in the CB of TiO_2 to ZnP^{2+} , which may be caused by the larger orbital distribution on the thiazolocatechol group than the carboxyphenyl group in HOMOs (Figure S7), and/or to the oxidized redox shuttle in the case of **ZnPTC**. In addition, we evaluated current-voltage curves in dark conditions (Figure S15). The onset voltage of the DSSC with **ZnPTC** is shifted to a negative direction by ca. 0.15 V relative to that with **YD2-o-C8**. This suggests the faster CR from the electrons in the CB of TiO_2 to the oxidized redox couple in the electrolyte solution for the DSSC with **ZnPTC** than that with **YD2-o-C8**. We have demonstrated that with an increase in the length of linkers between a porphyrin core and TiO_2 , the porphyrin tends to be inclined to TiO_2 , leading to fast CR on the time region of pico- and nanosecond and in turn low photovoltaic performances.^[15] More tilted geometry of **ZnPTC** than **YD2-o-C8** as the result of the longer linker of **ZnPTC** than **YD2-o-C8** together with the unfavorable orbital distribution of **ZnPTC** in HOMO would result in the plausible occurrence of the fast CR even on the time region of pico- and nanosecond, in addition to the microsecond region, and the eventual decrease in the V_{OC} and η_{col} values. Consequently, these fast CR processes together with the slow electron injection lower the ϕ_{inj} and η_{col} values, resulting in the moderate J_{SC} and η of the DSSC with **ZnPTC**.

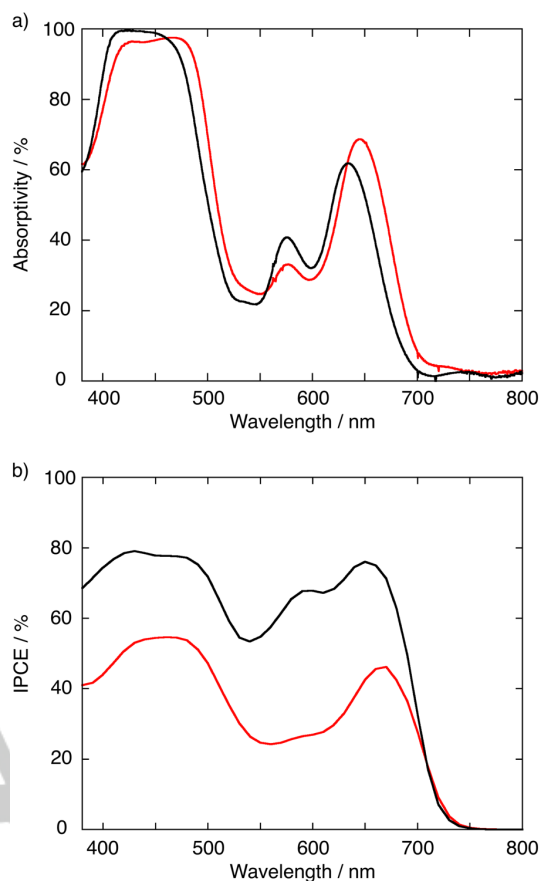


Figure 5. a) UV-Visible absorption spectra of the porphyrin-adsorbed TiO_2 electrodes with **YD2-o-C8** (black) and **ZnPTC** (red). Light-scattering TiO_2 layers were not used to obtain an accurate absorption profile. b) Plots of IPCE versus wavelength: DSSCs with **YD2-o-C8** (black) and **ZnPTC** (red) in the best conditions for achieving the highest η -values.

Long-term durability

We investigated the binding stability of **YD2-o-C8** and **ZnPTC** on TiO_2 . The porphyrin-sensitized TiO_2 electrodes were immersed in a THF- H_2O mixture ($v/v = 1:1$) containing 28 mM acetic acid or 0.1 mM NaOH. The amount of dye retained on TiO_2 was determined versus the immersion time from the absorbance of the TiO_2 electrode (Figure S16). After immersion in 8 h, the **YD2-o-C8** molecules were dissociated from TiO_2 by 70% and 100%, under acidic and alkaline conditions, respectively. In contrast, the **ZnPTC** molecules were detached from TiO_2 by 10% and 29% under the respective conditions. We also investigated the binding ability in organic and aqueous solutions without acetic acid or NaOH (Figure S17). **ZnPTC** showed no desorption under both conditions, whereas the **YD2-o-C8** molecules were desorbed from TiO_2 under the aqueous conditions. These results demonstrate the superior binding ability of the thiazolocatechol anchoring group to the carboxylic acid anchoring group. Then, we evaluated the long-term durability of DSSCs with **ZnPTC** and **YD2-o-C8** under continuous white light illumination (100 mW cm^{-2}) and dark conditions at 25 $^\circ\text{C}$ (Figure S18). Unfortunately, both cells exhibited similar decreasing profiles in the η -values

with increasing the illumination time despite the superior binding ability of **ZnPtc**. On the other hand, the **ZnPtc**-based DSSC showed almost no decrease in the η -value over 500 h, whereas the **YD2-o-C8**-based DSSC revealed a decrease of 16% in 500 h. Although the long-term durability under white light illumination is not improved for **ZnPtc**, the superior binding ability and cell durability under dark conditions signify the potential utility of the thiazolocatechol anchoring group for sensitizers in DSSCs.

Conclusions

We designed and synthesized a push-pull porphyrin sensitizer **ZnPtc** with a thiazolocatechol anchoring group to evaluate the effect of the thiazolocatechol group on the photovoltaic properties and long-term durability. The DSSC with **ZnPtc** exhibited the moderate photovoltaic performance ($\eta = 4.87\%$) compared to that with **YD2-o-C8** ($\eta = 9.93\%$). The moderate η -value for **ZnPtc** can be ascribed to the low ϕ_{nj} and η_{col} values from the unfavorable orbital distribution of the thiazolocatechol anchoring group on LUMO and HOMO as well as the fast CR from the electrons in the CB of TiO₂ to the oxidized redox couple in the electrolyte solution or to the oxidized porphyrin on TiO₂. Nevertheless, the photovoltaic performance of the DSSC with **ZnPtc** ($\eta = 4.87\%$) has overcome the barrier of $\eta = 4\%$ for the first time in catechol-based sensitizers. Therefore, fusion of the electron-withdrawing thiazole moiety with catechol was found to be effective to improve the photovoltaic performance of DSSCs. Moreover, we corroborated the superior binding ability of the thiazolocatechol anchoring group to the conventional carboxylic acid anchoring group under harsh conditions. We believe that further rational molecular design of catechol anchoring groups with a suitable electron-withdrawing moiety would make a breakthrough in DSSC sensitizers for achieving both high photovoltaic performances and long-term cell durability.

Experimental Section

Materials and Instruments: Commercially available reagents and solvents were employed without additional purification unless otherwise noted. Silica-gel column chromatography was carried out using UltraPure Silica Gel (230–400 mesh, SiliCycle) unless otherwise described. Thin-layer chromatography (TLC) was performed with Silica gel 60 F₂₅₄ (Merck). Size exclusion gel permeation chromatography (GPC) was implemented using Bio-beads S-X1 (Bio-rad). UV-visible-near infrared absorption and steady-state fluorescence spectra, ¹H and ¹³C NMR spectra, high-resolution mass spectra (HR-MS), and attenuated total reflectance-Fourier transform infrared (ATR-FTIR) spectra were recorded following the previously reported methods.^[6b] Electrochemical and X-ray photoelectron spectroscopy measurements were conducted according to our previous paper.^[6b] DFT calculations were carried out using the *Gaussian 09* program.^[16] All the structures of the porphyrins were fully optimized without any symmetry restriction at the B3LYP/6-31G(d) level for C, H, O, N, S, and Zn.

Synthesis: Porphyrin **5** was prepared according to literature.^[6b]

4-Nitro-1,2-phenylene diacetate (1): 4-Nitrocatechol (1.0 g, 6.4 mmol) and 4-dimethylaminopyridine (40 mg, 0.32 mmol, 5 mol%) were dissolved in dry THF (32 mL) and the mixed solution was cooled to 0 °C. Acetic anhydride was added to this solution and the solution was stirred at 0 °C. After 1 h, the reaction mixture was added to water and extracted with CH₂Cl₂, dried over anhydrous Na₂SO₄ and the solvent was evaporated under reduced pressure. The reaction mixture was purified by silica gel column chromatography using CH₂Cl₂ as eluent to give **1** as a white solid (1.5 g, 6.3 mmol, 98%). ¹H NMR^[17] (CDCl₃, 400 MHz): $\delta = 8.16$ (dd, $J = 8.8, 2.0$ Hz, 1H), 8.12 (d, $J = 7.6$ Hz, 1H), 7.40 (d, $J = 8.8$ Hz, 1H) and 2.34 (s, 6H) ppm.

4-Amino-1,2-phenylene diacetate (2): A solution of **1** (1.5 g, 6.3 mmol) in CHCl₃ (115 mL) was poured into a hydrogenator bomb and treated with 10 wt% Pd/C (401 mg). After 5 h, the reaction mixture was filtered on celite and the solvent was evaporated under reduced pressure. The crude product was purified by silica gel column chromatography using CH₂Cl₂/MeOH (v/v=50/1) as eluent to give **2** as a white solid (1.1 g, 5.3 mmol, 84%). ¹H NMR^[17] (CDCl₃, 400 MHz): $\delta = 6.93$ (d, $J = 8.4$ Hz, 1H), 6.52 (dd, $J = 8.6, 2.8$ Hz, 1H), 6.49 (d, $J = 2.8$ Hz, 1H), 3.68 (s, 2H), 2.26 (s, 3H) and 2.25 (s, 3H) ppm.

2-Amino-5,6-diacetoxymethylthiazole (3): To a solution of **2** (500 mg, 2.4 mmol) and KSCN (465 mg, 4.8 mmol, 2 eq.) in AcOH (12 mL), a solution of Br₂ (0.25 mL, 4.8 mmol, 2 eq.) in AcOH (12 mL) was added dropwise at room temperature. The mixture was stirred for 5.5 h at room temperature and then the reaction mixture was added to a saturated Na₂S₂O₃ aqueous solution and extracted with CH₂Cl₂, dried over anhydrous Na₂SO₄. After the solvent was evaporated under reduced pressure, the reaction mixture was purified by silica gel column chromatography using CH₂Cl₂/MeOH (v/v=100/1) as eluent to give **3** as a white solid (281 mg, 1.1 mmol, 46%). ¹H NMR (CDCl₃, 400 MHz): $\delta = 7.41$ (s, 1H), 7.33 (s, 1H), 5.24 (s, 1H), 2.31 (s, 3H) and 2.30 (s, 3H) ppm. ¹³C NMR (CDCl₃, 100 MHz): $\delta = 168.8, 168.7, 166.8, 150.5, 141.1, 137.7, 129.4, 115.3, 113.8$ and 20.8 ppm. FT-IR (ATR): $\nu = 2369, 2229, 2196, 2028, 1967, 1914, 1763, 1558, 1476, 1436, 1369, 1278, 1197, 1168, 1129, 1011, 967, 910$ and 871 cm⁻¹. MALDI-MS: m/z calcd for C₁₁H₁₀N₂O₄SNa: [M+Na]⁺ 289.0253; found 289.0251. m.p.: 162–164 °C.

2-Bromo-5,6-diacetoxymethylthiazole (4): To a solution of **3** (25 mg, 0.094 mmol) and CuBr (20 mg, 0.14 mmol, 1.5 eq.) in MeCN (1.3 mL) a solution of *tert*-butyl nitrite (90%, 17 μ L, 1.50 mmol) in MeCN (0.85 mL) was added dropwise at 0 °C. The mixture was stirred for 1 h at room temperature and then 3 h at 65 °C. The reaction mixture was added to water and extracted with EtOAc, washed with 1 M HCl aqueous solution, saturated NaHCO₃ aqueous solution, brine and water, dried over anhydrous Na₂SO₄. After the solvent was evaporated under reduced pressure, the reaction mixture was purified by silica gel column chromatography using CH₂Cl₂/MeOH (v/v=100/1) as eluent to give **4** as a white solid (25 mg, 0.076 mmol, 81%). ¹H NMR (CDCl₃, 400 MHz): $\delta = 7.81$ (s, 1H), 7.67 (s, 1H), 2.35 (s, 3H) and 2.33 (s, 3H) ppm. ¹³C NMR (CDCl₃, 100 MHz): $\delta = 168.4, 150.3, 141.7, 140.9, 140.2, 134.9, 117.3, 115.3, 20.8$ and 20.7 ppm. FT-IR (ATR): $\nu = 3439, 3039, 2531, 2422, 2156, 1760, 1646, 1535, 1459, 1372, 1209, 1190, 1137, 1016, 904$ and 867 cm⁻¹. MALDI-MS: m/z calcd for C₁₁H₉⁷⁹BrNO₄S: [M+H]⁺ 329.9430; found 329.9443. m.p.: 85–86 °C.

Porphyrin 6: Porphyrin **5** (0.060 mmol) was dissolved in a mixture of dry THF (11 mL) and NEt₃ (4.1 mL). To the mixture, **4** (100 mg, 0.30 mmol, 5.0 eq.), Pd₂(dba)₃ (69 mg, 0.075 mmol, 25 mol%) and AsPh₃ (150 mg, 0.48 mmol, 1.6 eq.) were added. The mixture was refluxed for 3 h under argon. Then, the reaction mixture was cooled to room temperature, washed with water, extracted with CH₂Cl₂, and dried over anhydrous Na₂SO₄. The solvent was evaporated under reduce pressure and the

reaction mixture was purified by silica gel column chromatography using CH_2Cl_2 as eluent and GPC using toluene as eluent to give **6** as a green solid (34 mg, 0.021 mmol, 35%). ^1H NMR (CDCl_3 , 400 MHz): δ = 9.66 (d, J = 4.4 Hz, 2H), 9.18 (d, J = 4.4 Hz, 2H), 8.90 (d, J = 4.4 Hz, 2H), 8.68 (d, J = 4.4 Hz, 2H), 8.02 (s, 1H), 7.83 (s, 1H), 7.66 (t, J = 8.4 Hz, 2H), 7.20 (d, J = 8.8 Hz, 4H), 6.95 (t, J = 9.2 Hz, 8H), 3.84 (t, J = 6.4 Hz, 8H), 2.46 (t, J = 7.8 Hz, 4H), 2.40 (s, 3H), 2.38 (s, 3H), 1.55–1.51 (m, 4H), 1.31–1.26 (m, 12H), 1.02–0.96 (m, 8H), 0.85–0.78 (m, 14H) and 0.65–0.45 (m, 44H) ppm. ^{13}C NMR (CDCl_3 , 100 MHz): δ = 168.5, 159.9, 152.4, 152.0, 151.7, 151.5, 150.8, 150.6, 141.9, 141.0, 134.9, 133.3, 133.0, 132.2, 131.0, 130.2, 130.1, 128.9, 124.6, 122.2, 120.5, 117.5, 115.4, 105.2, 102.8, 95.1, 88.6, 68.7, 35.4, 31.9, 31.7, 31.5, 29.3, 28.9, 28.7, 28.6, 25.3, 22.8, 22.4, 20.9, 20.8, 14.2 and 13.9 ppm. MALDI-MS: m/z calcd for $\text{C}_{101}\text{H}_{124}\text{N}_6\text{O}_8\text{S}_2\text{Zn}$: $[M]^+$ 1644.8487; found 1644.8504. FT-IR (ATR): ν = 3864, 3676, 3630, 3556, 2949, 2922, 2853, 2344, 2179, 2162, 1988, 1777, 1587, 1504, 1449, 1367, 1338, 1297, 1243, 1199, 1094, 996, 933, 910, 793 and 712 cm^{-1} . m.p.: 63 °C.

ZnPcTC: An aqueous solution of NaOH (20% w/w, 1.9 mL, 12 mmol) was added to a mixture of dry THF (2.0 mL) and MeOH (1.0 mL) containing porphyrin **6** (33 mg, 0.020 mmol). The solution was heated at 40 °C for 1 h. TLC (silica, CH_2Cl_2) showed complete hydrolysis of the ester. A saturated NH_4Cl aqueous solution was added to the reaction mixture and the mixture was diluted with CH_2Cl_2 , washed with brine, dried over anhydrous Na_2SO_4 . After the solvent was removed to give **ZnPcTC** as a green solid (31 mg, 0.020 mmol, quant.). ^1H NMR ($\text{CDCl}_3/\text{pyridine-}d_5$, 400 MHz): δ = 9.57 (d, J = 4.4 Hz, 2H), 9.00 (d, J = 4.4 Hz, 2H), 8.78 (d, J = 4.8 Hz, H), 8.57 (d, J = 4.4 Hz, 2H), 7.66 (s, 1H), 7.63 (t, J = 8.2 Hz, 2H), 7.39 (s, 1H), 7.00 (d, J = 8.0 Hz, 4H), 6.94 (d, J = 8.0 Hz, 4H), 6.80 (d, J = 8.4 Hz, 4H), 3.81 (t, J = 6.6 Hz, 8H), 2.40 (t, J = 7.6 Hz, 4H), 1.49–1.46 (m, 4H) and 0.93–0.42 (m, 78H) ppm. ^{13}C NMR ($\text{CDCl}_3/\text{pyridine-}d_5$, 100 MHz): δ = 160.0, 152.3, 151.5, 150.6, 150.4, 149.5, 149.1, 148.9, 135.8, 135.6, 135.4, 134.3, 132.2, 131.7, 130.5, 130.0, 129.7, 128.6, 123.5, 123.2, 123.0, 121.7, 121.4, 114.4, 107.8, 105.2, 105.1, 95.1, 88.7, 77.5, 77.4, 77.2, 76.8, 76.5, 68.6, 35.3, 31.8, 31.6, 31.1, 29.8, 29.3, 28.8, 28.72, 28.66, 25.2, 22.7, 22.4, 14.2 and 14.0 ppm. MALDI-MS: m/z calcd for $\text{C}_{97}\text{H}_{120}\text{N}_6\text{O}_6\text{S}_2\text{Zn}$: $[M]^+$ 1560.8276; found 1560.8247. FT-IR (ATR): ν = 3899, 3805, 3751, 3725, 3687, 3462, 2924, 2851, 2234, 2173, 2146, 2028, 1964, 1588, 1504, 1451, 1243, 1093, 995, 792 and 711 cm^{-1} . m.p.: 96–97 °C.

Photovoltaic Measurements: The TiO_2 electrodes and the sealed cells for photovoltaic measurements were prepared according to literatures.^[8b,12,18] The TiO_2 electrode was soaked into a THF/ethanol solution ($v/v = 1/4$) containing the porphyrins (0.20 mM) at 25 °C. The electrolyte solution consisted of 0.25 M $[\text{Co}(\text{bpy})_3](\text{TFSI})_2$, 0.05 M $[\text{Co}(\text{bpy})_3](\text{TFSI})_3$, 0.1 M lithium bis(trifluoromethanesulfonyl)imide (LiTFSI), and 0.5 M 4-*tert*-butylpyridine in acetonitrile. Photovoltaic measurements were conducted according to our previous papers.^[8b,11]

Acknowledgements

This work was supported by the JSPS (KAKENHI Grant Numbers JP18H03898 (H.I.) and JP18K14198(T.H.)). In this work, DFT calculations were performed by the supercomputer of ACCMS, Kyoto University.

Keywords: porphyrin • thiazole • catechol • solar cell • anchoring group

- [1] a) M. Grätzel, *Acc. Chem. Res.* **2009**, *42*, 1788–1798; b) A. Hagfeldt, G. Boschloo, L. Sun, L. Kloo, H. Pettersson, *Chem. Rev.* **2010**, *110*, 6595–6663; c) H. S. Jung, J.-K. Lee, *J. Phys. Chem. Lett.* **2013**, *4*, 1682–1693.
- [2] a) M. S. Prévot, K. Sivula, *J. Phys. Chem. C* **2013**, *117*, 17879–17893; b) J. R. Swierk, T. E. Mallouk, *Chem. Soc. Rev.* **2013**, *42*, 2357–2387; c) Z. Yu, F. Li, L. Sun, *Energy Environ. Sci.* **2015**, *8*, 760–775.
- [3] a) B. O'Regan, M. Grätzel, *Nature* **1991**, *353*, 737–740; b) M. K. Nazeeruddin, F. De Angelis, S. Fantacci, A. Selloni, G. Viscardi, P. Liska, S. Ito, T. Bessho, M. Grätzel, *J. Am. Chem. Soc.* **2005**, *127*, 16835–16847; c) F. Gao, Y. Wang, D. Shi, J. Zhang, M. Wang, X. Jing, R. Humphry-Baker, P. Wang, S. M. Zakeeruddin, M. Grätzel, *J. Am. Chem. Soc.* **2008**, *130*, 10720–10728; d) A. Abbotto, N. Manfredi, *Dalton Trans.* **2011**, *40*, 12421–12438; e) T. Kinoshita, J. T. Dy, S. Uchida, T. Kubo, H. Segawa, *Nat. Photonics* **2013**, *7*, 535–539; f) Z. She, Y. Cheng, L. Zhang, X. Li, D. Wu, Q. Guo, J. Lan, R. Wang, J. You, *ACS Appl. Mater. Interfaces* **2015**, *7*, 27831–27837.
- [4] a) A. Mishra, M. K. R. Fischer, P. Bäuerle, *Angew. Chem. Int. Ed.* **2009**, *48*, 2474–2499; *Angew. Chem.* **2009**, *121*, 2510–2536; b) Y. Ooyama, Y. Harima, *European J. Org. Chem.* **2009**, *2009*, 2903–2934; c) Y. Wu, W.-H. Zhu, S. M. Zakeeruddin, M. Grätzel, *ACS Appl. Mater. Interfaces* **2015**, *7*, 9307–9318; d) K. Kakiage, Y. Aoyama, T. Yano, K. Oya, J. Fujisawa, M. Hanaya, *Chem. Commun.* **2015**, *51*, 15894–15897; e) J. Wang, K. Liu, L. Ma, X. Zhan, *Chem. Rev.* **2016**, *116*, 14675–14725; f) H. Klifout, A. Stewart, M. Elkhalfia, H. He, *ACS Appl. Mater. Interfaces* **2017**, *9*, 39873–39889; g) P. Brogdon, H. Cheema, J. H. Delcamp, *ChemSusChem* **2018**, *11*, 86–103; h) Y. Ren, D. Sun, Y. Cao, H. N. Tsao, Y. Yuan, S. M. Zakeeruddin, P. Wang, M. Grätzel, *J. Am. Chem. Soc.* **2018**, *140*, 2405–2408.
- [5] a) H. Imahori, T. Umeyama, S. Ito, *Acc. Chem. Res.* **2009**, *42*, 1809–1818; b) L.-L. Li, E. W.-G. Diau, *Chem. Soc. Rev.* **2013**, *42*, 291–304; c) M. Urbani, M. Grätzel, M. K. Nazeeruddin, T. Torres, *Chem. Rev.* **2014**, *114*, 12330–12396; d) T. Higashino, H. Imahori, *Dalton Trans.* **2015**, *44*, 448–463; e) H. Song, Q. Liu, Y. Xie, *Chem. Commun.* **2018**, *54*, 1811–1824; f) J.-M. Ji, H. Zhou, H. K. Kim, *J. Mater. Chem. A* **2018**, *6*, 14518–14545.
- [6] a) T. Bessho, S. M. Zakeeruddin, C.-Y. Yeh, E. W.-G. Diau, M. Grätzel, *Angew. Chem. Int. Ed.* **2010**, *49*, 6646–664; *Angew. Chem.* **2010**, *122*, 6796–6799; b) A. Yella, H.-W. Lee, H. N. Tsao, C. Yi, A. K. Chandiran, M. K. Nazeeruddin, E. W.-G. Diau, C.-Y. Yeh, S. M. Zakeeruddin, M. Grätzel, *Science* **2011**, *334*, 629–634; c) K. Kurotobi, Y. Toude, K. Kawamoto, Y. Fujimori, S. Ito, P. Chabera, V. Sundström, H. Imahori, *Chem. Eur. J.* **2013**, *19*, 17075–17081; d) A. Yella, C.-L. Mai, S. M. Zakeeruddin, S.-N. Chang, C.-H. Hsieh, C.-Y. Yeh, M. Grätzel, *Angew. Chem. Int. Ed.* **2014**, *53*, 2973–2977; *Angew. Chem.* **2014**, *126*, 3017–3021; e) S. Mathew, A. Yella, P. Gao, R. Humphry-Baker, B. F. E. Curchod, N. Ashari-Astani, I. Tavernelli, U. Rothlisberger, M. K. Nazeeruddin, M. Grätzel, *Nat. Chem.* **2014**, *6*, 242–247; f) Y. Xie, Y. Tang, W. Wu, Y. Wang, J. Liu, X. Li, H. Tian, W.-H. Zhu, *J. Am. Chem. Soc.* **2015**, *137*, 14055–14058; g) S. H. Kang, M. J. Jeong, Y. K. Eom, I. T. Choi, S. M. Kwon, Y. Yoo, J. Kim, J. Kwon, J. H. Park, H. K. Kim, *Adv. Energy Mater.* **2017**, *7*, 1602117; h) Y. Lu, H. Song, X. Li, H. Ågren, Q. Liu, J. Zhang, X. Zhang, Y. Xie, *ACS Appl. Mater. Interfaces* **2019**, *11*, 5046–5054.
- [7] a) S. P. Pujari, L. Scheres, A. T. M. Marcellis, H. Zuilhof, *Angew. Chem. Int. Ed.* **2014**, *53*, 6322–6356; *Angew. Chem.* **2014**, *126*, 6438–6474; b) L. Zhang, J. M. Cole, *ACS Appl. Mater. Interfaces* **2015**, *7*, 3427–3455.
- [8] a) T. Higashino, Y. Fujimori, K. Sugiura, Y. Tsuji, S. Ito, H. Imahori, *Angew. Chem. Int. Ed.* **2015**, *54*, 9052–9056; *Angew. Chem.* **2015**, *127*, 9180–9184; b) T. Higashino, Y. Kurumisawa, N. Cai, Y. Fujimori, Y. Tsuji, S. Nimura, D. M. Packwood, J. Park, H. Imahori, *ChemSusChem* **2017**, *10*, 3347–3351.
- [9] a) I. A. Janković, Z. V. Šaponjić, M. I. Čomor, J. M. Nedeljković, *J. Phys. Chem. C* **2009**, *113*, 12645–12652; b) Y. Ooyama, T. Yamada, T. Fujita, Y. Harima, *J. Mater. Chem. A* **2014**, *2*, 8500–8511.

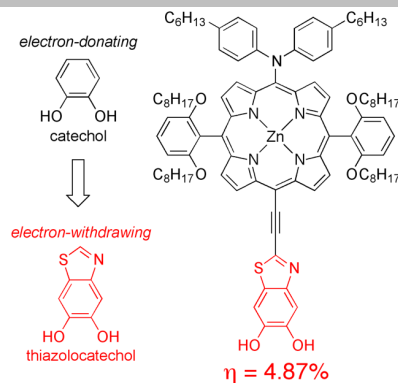
- [10] a) E. L. Tae, S. H. Lee, J. K. Lee, S. S. Yoo, E. J. Kang, K. B. Yoon, *J. Phys. Chem. B* **2005**, *109*, 22513–22522; b) B. An, W. Hu, P. L. Burn, P. Meredith, *J. Phys. Chem. C* **2010**, *114*, 17964–17974; c) Y. Ooyama, M. Kanda, K. Uenaka, J. Ohshita, *ChemPhysChem* **2015**, *16*, 3049–3057; d) Y. Ooyama, K. Furue, T. Enoki, M. Kanda, Y. Adachi, J. Ohshita, *Phys. Chem. Chem. Phys.* **2016**, *18*, 30662–30676; e) M. Adineh, P. Tahay, M. Ameri, N. Safari, E. Mohajerani, *RSC Adv.* **2016**, *6*, 14512–14521.
- [11] P. Piatkowski, C. Martin, M. R. di Nunzio, B. Cohen, S. Pandey, S. Hayse, A. Douhal, *J. Phys. Chem. C* **2014**, *118*, 29674–29687.
- [12] T. Higashino, Y. Kurumisawa, H. Iiyama, H. Imahori, *Chem. Eur. J.* **2019**, *25*, 538–547.
- [13] a) H. Imahori, Y. Matsubara, H. Iijima, T. Umeyama, Y. Matano, S. Ito, M. Niemi, N. V. Tkachenko, H. Lemmetyinen, *J. Phys. Chem. C* **2010**, *114*, 10656–10665; b) T. Higashino, Y. Fujimori, K. Sugiyama, Y. Tsuji, S. Ito, H. Imahori, *J. Porphyrin Phthalocyanines* **2015**, *19*, 140–149.
- [14] A. Kira, Y. Matsubara, H. Iijima, T. Umeyama, Y. Matano, S. Ito, M. Niemi, N. V. Tkachenko, H. Lemmetyinen, H. Imahori, *J. Phys. Chem. C* **2010**, *114*, 11293–11304.
- [15] a) H. Imahori, S. Kang, H. Hayashi, M. Haruta, H. Kurata, S. Isoda, S. E. Canton, Y. Infahsaeng, A. Kathiraven, T. Pascher, P. Chábera, A. P. Yartsev, V. Sundström, *J. Phys. Chem. A* **2011**, *115*, 3679–3690; b) S. Ye, A. Kathiravan, H. Hayashi, Y. Tong, Y. Infahsaeng, P. Chabera, T. Pascher, A. P. Yartsev, S. Isoda, H. Imahori, *J. Phys. Chem. C* **2013**, *117*, 6066–6080.
- [16] Gaussian 09, Revision D.01, M. J. Frisch, G. W. Trucks, H. B. Schlegel, G. E. Scuseria, M. A. Robb, J. R. Cheeseman, G. Scalmani, V. Barone, B. Mennucci, G. A. Petersson, H. Nakatsuji, M. Caricato, X. Li, H. P. Hratchian, A. F. Izmaylov, J. Bloino, G. Zheng, J. L. Sonnenberg, M. Hada, M. Ehara, K. Toyota, R. Fukuda, J. Hasegawa, M. Ishida, T. Nakajima, Y. Honda, O. Kitao, H. Nakai, T. Vreven, J. A. Montgomery, Jr., J. E. Peralta, F. Ogliaro, M. Bearpark, J. J. Heyd, E. Brothers, K. N. Kudin, V. N. Staroverov, T. Keith, R. Kobayashi, J. Normand, K. Raghavachari, A. Rendell, J. C. Burant, S. S. Iyengar, J. Tomasi, M. Cossi, N. Rega, J. M. Millam, M. Klene, J. E. Knox, J. B. Cross, V. Bakken, C. Adamo, J. Jaramillo, R. Gomperts, R. E. Stratmann, O. Yazyev, A. J. Austin, R. Cammi, C. Pomelli, J. W. Ochterski, R. L. Martin, K. Morokuma, V. G. Zakrzewski, G. A. Voth, P. Salvador, J. J. Dannenberg, S. Dapprich, A. D. Daniels, O. Farkas, J. B. Foresman, J. V. Ortiz, J. Cioslowski, D. J. Fox, Gaussian, Inc.; Wallingford CT, **2013**.
- [17] L. Capelli, P. Manini, A. Pezzella, A. Napolitano, M. d'Ischia, *J. Org. Chem.* **2009**, *74*, 7191–7194.
- [18] S. Ito, T. N. Murakami, P. Comte, P. Liska, C. Grätzel, M. K. Nazeeruddin, M. Grätzel, *Thin Solid Films* **2008**, *516*, 4613–4619.

Entry for the Table of Contents (Please choose one layout)

Layout 1:

FULL PAPER

We designed and synthesized a push-pull porphyrin sensitizer **ZnP_{TC}** with a thiazolocatechol as a catechol anchoring group with an electron-withdrawing thiazole moiety. The dye-sensitized solar cell with **ZnP_{TC}** revealed an energy conversion efficiency of 4.87%, exceeding the barrier of 4% for the first time in catechol-based sensitizers.



T. Higashino, H. Iiyama, Y. Kurumisawa, H. Imahori*

Page No. – Page No.

Thiazolocatechol: Electron-withdrawing Catechol Anchoring Group for Dye-Sensitized Solar Cells

Layout 2:

FULL PAPER

((Insert TOC Graphic here; max. width: 11.5 cm; max. height: 2.5 cm))

Author(s), Corresponding Author(s)*

Page No. – Page No.

Title

Text for Table of Contents